Vol.8, No.2 pages 1-16 Science Technology and Engineering Journal (STEJ) Research Article

First cytogenomic characterization of murine cutaneous sarcoma cell line TSC2ang1

Shaymaa Azawi[1], Fritz Kramer[1], Thomas Liehr[1*], Martina Rincic[2]

[1] *Jena University Hospital, Friedrich Schiller University, Institute of Human Genetics, Am Klinikum 1, D-07747 Jena, Germany*

[2] *Croatian Institute for Brain Research, School of Medicine University of Zagreb, Salata 12, 10000 Zagreb, Croatia;*

[*] *Thomas Liehr: Thomas.Liehr@med.uni-jena.de*

(**Received**: 23rd May 2022, **Received**: 18th July 2022, **Accepted**: 19th July 2022)

Abstract - The murine cutaneous sarcoma cell line TSC2ang1 has been established in 1999 and recently been suggested to be a model for tuberous sclerosis-associated skin lesions/ hamartomas. This suggestion was founded in first place on the fact that the cell line has been established from tumor arising in a heterozygote tsc2-gene knockout mouse. Here, as the genetic characteristics of TSC2ang1 have never been determined in detail before, chromosome microarray and multicolor banding-based molecular cytogenetics were done. A near tetraploid karyotype with 69 to 77 chromosomes per cell, and two equally sized subclones were characterized for TSC2ang1. Into the human genome translated results of identified gains and losses, and a literature review showed that TSC2ang1 is rather suited as a sarcoma model than for tuberous sclerosis-associated hamartomas.

Keywords: Murine tumor cell line, sarcoma, tuberous sclerosis, hamartomas, molecular cytogenetics.

1. Introduction

Patients with tuberous sclerosis (TS) are in most cases already diagnosed in newborn age, as they suffer from a multisystem disorder; however, signs and symptoms can be variable. Nonetheless, an early diagnosis is imperative for the patient's adequate treatment, as they may develop benign tumors-called hamartomas-in different organ systems like skin, brain, eyes, heart, kidneys and lungs. These tumors are often referred to as hamartomas, which do not typically metastasize but can nonetheless harm surrounding normal tissues (Swarbrick *et al.*, 2021; Wlodarski *et al.*, 2008). TS is following an autosomal dominant trait, shows up most often de novo, and is caused by mutation in tumor suppressor gene TSC1 in 9q34.31 (coding for hamartin; chr9[GRCh37/hg19] 135,766,735-135,820,020) (Van Slegtenhorst *et al.*, 1997) or TSC2 in 16p13.3 (coding for tuberin; chr16[GRCh37/hg19] 2,097,990-2,138,713) (European Chromosome 16 Tuberous Sclerosis Consortium, 1993). TSC1 or TSC2 gene mutations lead to cell cycle progression and oncogenic transformation, as (via different metabolic steps) they interfere with and activate the mTOR pathway (Luo *et al.*, 2022).

As besides patient biopsies cellular models for in vitro studies are scares, TSC2ang1, a murine TS-associated line was recently brought back to mind of TS-researchers (Wlodarski *et al.*, 2008). Wlodarski *et al.* (2008) determined chromosome numbers of TSC2ang1 as 71~74 and detected one and two Robertsonian translocations in 48% and 6% of metaphase plates, each. Besides, no cytogenetic or cytogenomic study was available yet for this in 1999 first published cell line (Onda *et al.*, 1999). TSC2ang1 was established from a cutaneous invasive sarcoma which developed in a Tsc2+/-mouse (Mus musculus f. domestica) heterozygous for tuberin (Onda *et al.*, 1999). Since then it has been applied only in few studies (Gao *et al.*, 2015; Govindarajan *et al.*, 2012; Alesi *et al.*, 2021; Ferreira *et al.*, 2017; Alkharusi *et al.*, 2016). Here we present the first comprehensive cytogenomic characterization of TSC2 ang 1 using murine multicolor banding (mcb) combined with molecular karyotyping; the detected imbalances were in silico translated into the human genome (as previously described Kubicova *et al.* (2017)) and revealed that TSC2ang1 shows a typical sarcoma imbalance pattern; thus, it is unlikely to be a model for tuberous sclerosis-associated skin lesions/ hamartomas.

2. Materials and methods

2.1 Cell line work up and molecular (cyto)genetics

After adherent cultivation of murine TSC2ang1 cell line acc. to provider's instructions (American Typed Culture Collection, ATCCR CRL-2620™; Wesel Germany), cells were prepared in parallel cytogenetically to get chromosomes, and molecular genetically to extract whole genomic DNA (Kubicova *et al.*, 2017).

As previously described fluorescence in situ hybridization (FISH) was done: for multicolor-FISH (mFISH) whole chromosome paints ("SkyPaintTM DNA Kit M-10 for Mouse Chromosomes", Applied Spectral Imaging, Edingen-Neckarhausen, Germany), and for FISH-banding murine chromosome-specific multicolor banding (mcb) probe mixes (Kubicova *et al.*, 2017) were used. At least 30 metaphases were

analyzed for each probe set (Zeiss Axioplan microscopy, equipped with ISIS software (MetaSystems, Altlussheim, Germany). Chromosome microarray studies (CMA) were performed by "SurePrint G3 Mouse CGH Microarray, 4×180K" (Agilent Technologies, Waldbronn, Germany) (Kubicova *et al.*, 2017).

Imbalances and breakpoints of TSC2ang1 according to mcb and CMA data, were aligned to human homologous regions using Ensembl and the UCSC Genome Browser, as previously done (Kubicova *et al.*, 2017). The obtained data was compared to genetic changes known from human sarcomas (Forus *et al.*, 1995; Mihic-Probst *et al.*, 2004; Deeb *et al.*, 2005).

2.2 Ethics statement

According to the ethical committee (medical faculty) and the Animal Experimentation Commission of the Friedrich Schiller University, there are no ethical agreements necessary for studies involving murine tumor cell lines like TSC2ang1.

3. Results

The TSC2ang1 cell line is near tetraploid, has two X-chromosomes (Figure 1) and it is not clear if two Y-or two X-chromosomes were lost during cultivation, as the gender of original mouse was reported. The cell line fell into two related clones of approximately equal sizes. Clone 1 had a karyotype of 72-77<4n>,XX,-2,del(4)(C1),+del(4)(C1),+del(4)(C1),del(5)(C1G2),del(6)(B3),-7,del(8)(C5),-9,-11,-14,-16 and clone 2 of 69~74<4n>,XX,-2,der(4)t(4;5)(E2B2),-4,del(5)(C1G2),del(6)(B3),-7,del(8)(C5),-9,idic(11)(A),inv dup(13)(C2),-14,dic(16,18)(A1;A1). In Figure 1A clone 1 is shown and in Figure 1B only the changes present in clone 2 compared to clone 1.

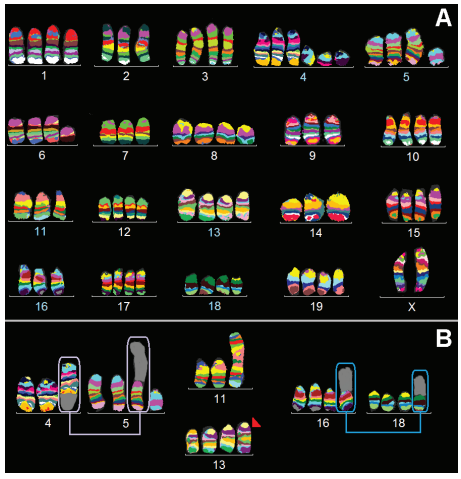

Figure 1. Pseudo-color banding depiction of 20 chromosome-specific murine multicolor banding experiments applied in murine cutaneous sarcoma cell line TSC2ang1. In (A) all (derivative) chromosomes are 1 depicted for clone 1; those six chromosomes which showed different aberrations in clone 2 are highlighted by light-blue chromosome-numbers. In (B) only those six chromosomes, i.e. 4, 5, 11, 13, 16 and 18, are depicted, which were different in clone 2 compared to clone 1. Here also derivative chromosomes consisting of different chromosomes are highlighted by frames and displayed twice. The derivative chromosome inv dup(13)(C2) is highlighted by a red arrowhead.

In Figure 2A the results of CMA for TSC2ang1 cell line are summarized; these results are translated into the human genome in Figure 2B and Table 1. It is visible in Table 1 that the tsc2 gene may be deleted in clone 2 due to the dic(16;18) formation. Besides it is reported tsc2 has been also knocked in the original mouse model, but this deletion is most likely too small to be detectable in CMA.

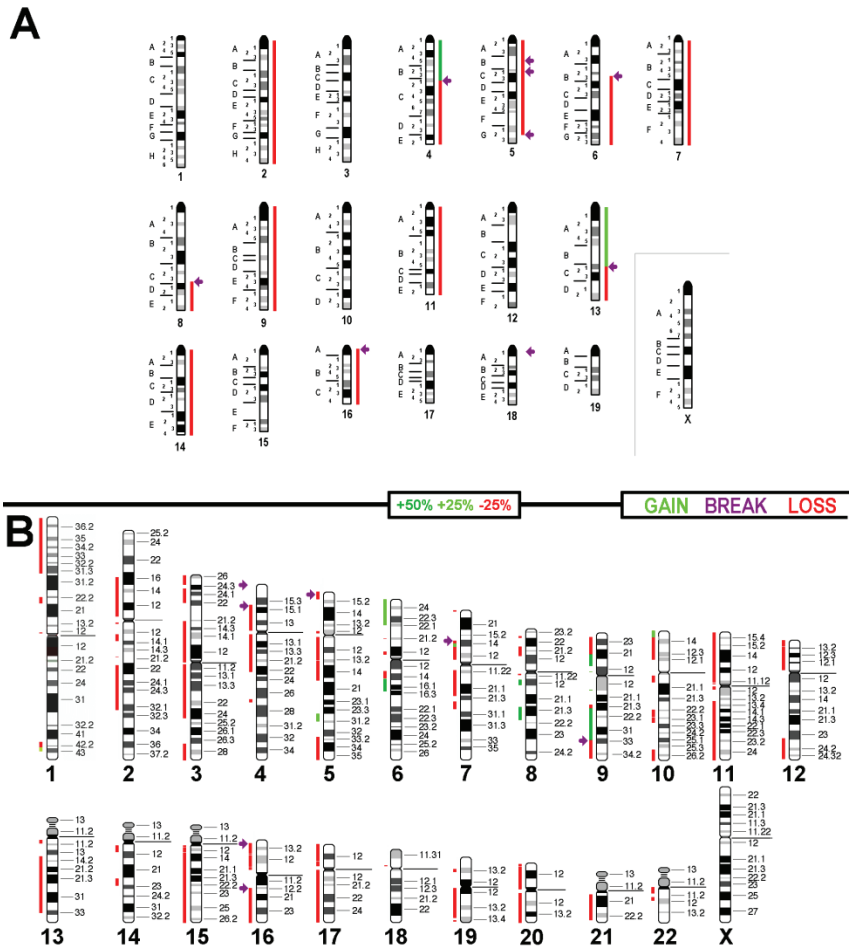

Figure 2. Chromosome microarray (CMA) results of TSC2ang1 cell line is depicted with respect to a diploid-basic karyotype. Gains are indicated as green bars, losses in red and breaks with arrows. (A) Imbalances observed in the cell line depicted along a murine chromosome set. (B) Results translated and projected along the human chromosome set.

The translation of detected imbalances in TSC2ang1 (Figure 2A) into the human genome (Fig 2B, Table 1) enabled a comparison with imbalances present in human sarcomas.

Table 1. The regions of gain and loss of copy numbers, as well of breakpoints of balanced rearrangements, observed in TSC2ang1 and the corresponding homologue regions in humans, are listed as cytoband and position (GRCh37/hg19).

region	gain	homologue region in human	
		cytoband	position (GRCh37/hg19)
4A1-C1	+2 copies (clone 1)	8q12.1-q12.3	8:56650304-62695565
		8q21.3-q22.1	8:87057363-97246782
		8q12.3	8:63094926-64018516
		6q14.3-q16.2	6:87793887-100245013
		9p21.2-p13.1	9:27325073-38472099
		9q22.33-q33.2	9:100037894-122653620
13A-C1	+1 copy (clone 2)	10p15.3-p15.1	10:138698-5865622
		1q42.3-q43	1:235330060-240084659
		7p14.2-p13	7:36524506-43605930
		6p22.3-p22.1	6:20065223-28502803
		6p25.3-p23	6:181261-15099150
		6p23-p22.3	6:15104709-20060798
		9q22.1-q22.32	9:91031851-97067712
		5q35.2-q35.3	5:173750964-177039611
		5q31.1-q31.2	5:134073478-137090938
		9q21.32-q21.33	9:86231955-90340399
		9q22.32-q22.33	9:97320957-99417669
		9p13.1	9:38810965-40707569
		9q12-q13	9:65585614-65901647
		9p11.2	9:43623473-43941731
		8q22.1	8:97247028-97373828
		5p15.33-p15.32	5:191425-5575825
2A-qter	-1 copy	10p15.1-p12.1	10:5915452-27157072
		10p12.1	10:27398972-27531240
		2q22.1	2:138721435-139545160
		2q13	2:113723845-114137444
		9q34.11-q34.3	9:131071714-141019156
		9q33.2-q34.11	9:123526077-131061546
		2q22.1-q32.1	2:140065297-188395329
		11q12.1	11:56082416-57753858
		11q11	11:55080583-55323018
		11p11.12	11:51377850-51539057
		11p14.2-p11.2	11:26296397-48658712
		15q13.3-q21.2	15:32906987-51298173
		2q11.1-q11.2	2:95642277-97040617
		2q13	2:111483204-112960231
		2p11.2	2:87345633-87996071
		2q13	2:112973390-113650007
		20p13-p11.21	20:1736101-25606620
		20p13	20:102147-1447942
		20q11.21-q13.32	20:29933153-58056214
		20q13.32-q13.33	20:58148222-62907435

Table 1. The regions of gain and loss of copy numbers, as well of breakpoints of balanced rearrangements, observed in TSC2ang1 and the corresponding homologue regions in humans, are listed as cytoband and position (GRCh37/hg19). (cont.)

region	gain	homologue region in human	
		cytoband	position (GRCh37/hg19)
4C1-qter	-1 copy (clone 2)	9q33.2	9:122653620-123488942
		9q21.31-q21.32	9:82993521-85697078
		9q21.32	9:85856924-86154717
		9p24.1-p21.2	9:6847129-27220407
		1p32.1-p31.3	1:59120351-67562260
		1p36.33-p32.2~1	1:894315-59012766
5C1-G2	-1 copy	4p15.2-p11	4:21980336-49083612
		4q12-q22.1	4:52689038-89000187
		1p22.2-p22.1	1:89950168-93744300
		4p16.3	4:493106-1023731
		12q24.33	12:132378991-133522542
		22q11.23-q12.1	22:25201765-29156283
		12q23.3-q24.11	12:108325357-110486420
		12q24.11-q24.31	12:110488793-121497537
		12q24.31-q24.33	12:121577100-132336561
		7p11.2	7:56019352-56184138
		7q11.21-q11.22	7:66808098-72045725
		7q11.23	7:72536306-76149827
		7q22.1	7:99552841-102191754
		7p22.3-p22.1	7:115497-5047829
6B3-qter	-1 copy	7p14.3	7:31961393-33103246
		4q22.1-q22.3	4:89178698-95273100
		4q27	4:121018693-122194687
		1p31.3	1:67631910-68317098
		2p11.2	2:88302422-89174373
		2p13.3-p11.2	2:68715037-87095119
		3q21.2-q21.3	3:125725101-129038484
		3p25.2-p25.1	3:12939278-15163105
		3p14.1-p12.3	3:64017713-75322601
		3p26.3-p25.2	3:61304-12897767
		3q21.3-q22.1	3:129094932-129632650
		10q11.21-q11.22	10:43277986-46218167
		12p13.33	12:66113-2823666
		22q11.1-q11.21	22:17565811-18659740
		12p13.31	12:8071763-9214464
		12p13.33-p13.31	12:2903120-7695890
		12p11.21	12:30985917-31165338
		12p13.31-p11.21	12:9901365-30943693
		12p11.21	12:31424829-32537434

Table 1. The regions of gain and loss of copy numbers, as well of breakpoints of balanced rearrangements, observed in TSC2ang1 and the corresponding homologue regions in humans, are listed as cytoband and position (GRCh37/hg19). (cont.)

region	gain	homologue region in human	
		cytoband	position (GRCh37/hg19)
7A-qter	-1 copy	19q13.42-q13.43	19:54368915-57485284
		19q13.43	19:58523795-59089552
		19q13.31-q13.33	19:45010010-48707700
		19q12-q13.31	19:30093064-44860951
		19q12	19:28589680-30085362
		19q13.33-q13.41	19:48800017-51921957
		16p13.11	16:16252815-16388674
		11p15.1-p14.3	11:17403485-25251145
		15q11.2	15:22833222-23086601
		15q11.2-q13.1	15:23914751-28586067
		15q13.1-q13.3	15:29107424-32578594
		15q26.3	15:99080385-102265870
		15q26.1-q26.3	15:91593058-99078056
		15q25.3-q26.1	15:85829657-91565912
		15q25.1-q25.3	15:80253398-85682414
		11p11.12	11:49250334-49827246
		11q13.4-q14.3	11:71627032-89350901
		10p11.21	10:37191655-37402201
		11p15.4-p15.1	11:3631069-17360027
		16p13.11	16:15260325-15369270
		16p13.11-p12.3	16:16681590-18325190
		16p12.3-p12.2	16:18608156-21351663
		16p12.2-p11.2	16:21572755-28339524
		16p11.2	16:28390845-29030948
		16p11.2	16:29661006-31520748
		10q26.11-q26.3	10:121224592-135295738
		11p15.5-p15.4	11:192898-3098752
		11q13.3-q13.4	11:68728143-71212974
8C5-qter	-1 copy	16q12.2-q22.1	16:56003242-69976105
		16q22.1-q24.3	16:70109527-90110030
		1q42.13-q42.3	1:229404294-235324774
		10p11.22-p11.21	10:33112469-35152269
9A-qter	-1 copy	11q14.3-q22.3	11:89860533-107436639
		19p13.2	19:8919008-11689880
		7p14.3-p14.2	7:33134362-36494039
		11q22.3-q25	11:107452617-134843539
		15q21.2	15:51349622-51942502
		15q21.2-q25.1	15:51961808-78956872
		6p12.2-p12.1	6:52656530-55784577
		6q13-q14.3	6:74104388-86360515
		15q25.1	15:79042978-80196839
		3q22.3-q24	3:138372654-148087492
		3q22.1-q22.3	3:129931635-138353358
		3p21.31-p21.1	3:46446256-52346387
		3p24.1-p22.2	3:27753690-37261140
		3p22.2-p21.31	3:37269243-46423369

Table 1. The regions of gain and loss of copy numbers, as well of breakpoints of balanced rearrangements, observed in TSC2ang1 and the corresponding homologue regions in humans, are listed as cytoband and position (GRCh37/hg19). (cont.)

region	gain	homologue region in human	
		cytoband	position (GRCh37/hg19)
11A-qter	-1 copy (clone 1)	22q12.1-q12.2	22:29251511-32022116
		7p13-p11.2	7:43906144-55317931
		2p16.2-p14	2:53882943-68694726
		5q35.1-q35.2	5:172736725-173663599
		5q33.2-q35.1	5:154331837-171932313
		5q35.3	5:177531363-180585244
		5q23.3-q31.1	5:130484032-134063627
		5q33.1-q33.2	5:150381711-154330989
		1q42.13	1:227919753-228703212
		17p11.2	17:16917258-21343117
		17p12-p11.2	17:15731601-16472951
		17p13.3-p12	17:2-15625804
		17q11.1-q11.2	17:25525650-28853901
		17q11.2-q12	17:29058377-36200511
		17q21.32-q23.2	17:45560334-60326198
		17q12-q21.31	17:36351926-43638822
		17q21.31-q21.32	17:43706746-45150591
		17q21.32	17:45188646-45518436
		17q23.2-q24.1	17:60483588-62760387
		17q24.1-q24.2	17:62990972-66110690
		17q24.2-q25.3	17:66224207-81175056
13C1-qter	-1 copy (clone 2)	5p15.32-p15.31	5:5575825-7935441
		5q14.3-q15	5:84566270-96144383
		5q13.2-q14.3	5:70265557-84371909
		5q11.1-q13.2	5:49569996-68922426
		1p11.2	1:121149401-121350677
		5p12	5:43446298-46118514
14A-qter	1x	3p14.3-p14.1	3:57993765-64009700
		3p24.3-p24.1	3:23146386-27721393
		14q22.1	14:52272055-52598781
		6p21.2	6:39069766-39266486
		10q22.1-q22.3	10:74870164-81255099
		3p21.1-p14.3	3:52350060-57931230
		3p25.1	3:15245114-16307845
		10q11.2-q11.23	10:46488677-51727392
		10q23.1-q23.2	10:82019368-88976316
		14q22.1-q23.1	14:52688635-58629894
		14q11.2-q12	14:20211286-24987352
		14q12	14:25040539-25149959
		13q12.12	13:25188452-25511922
		13q12.11	13:20207279-23370461
		13q14.2	13:49821990-50161404
		13q12.13	13:25685086-26668986
		13q12.12	13:23853398-24896355
		13q14.2-q14.3	13:50192169-52356487
		8p23.1	8:9744629-11737304
		8p21.3-p12	8:20206584-29151199
		13q14.11-q14.2	13:41469941-49799059
		13q14.3-q33.1	13:53226033-103089581

Table 1. The regions of gain and loss of copy numbers, as well of breakpoints of balanced rearrangements, observed in TSC2ang1 and the corresponding homologue regions in humans, are listed as cytoband and position (GRCh37/hg19). (cont.)

region	gain	homologue region in human	
		cytoband	position (GRCh37/hg19)
16A-qter	1x (clone 1)	16p13.3-p13.11	16:3283710-15197331
		16p13.11	16:15478874-16187414
		8q11.21	8:48206338-49865275
		12p11.21	12:32634919-33054761
		22q11.21	22:19010381-22338262
		3q27.1-q29	3:182965714-195325931
		3q29	3:195428230-197771581
		3q11.1-q21.2	3:93527487-125343459
		3p12.3-p11.1	3:75865702-90309600
		21q11.2-q22.3	21:15515528-43438088
		21q11.2	21:14535253-14714360
		18p11.21	18:15016525-15155234
		2q21.1	2:132604281-132757591
4C1	del	9q33.2	9:123151147-123342448 (CDK5RAP2)
5B2	t	4p16.3	4:3294755-3441640 (RGS12)
5C1	del	4p15.2	4:25749055-25865382 (SEL1L3)
5G2	del	no homologous	
6B3	del	7p14.3	7:31553704-31698334 (CCDC129)
8C5	del	16q12.2	16:56225302-56391356 (GNAO1)
11A1	idic	22q12.2	22:31884674-32014572 (SFI1)
13C1	dup	5p15.33	5:2745959-2752969 (IRX2
16A1	dic	16p13.3	16:3254247-3255188 (OR1F1)
18A1	dic	16p13.3	16:1413206-1464752 (UNKL)

No CMA data was available for hamartomas, but comparison of TSC2ang1 with undifferentiated high grade pleomorphic and myeloid sarcoma revealed a 55-58% concordance for the gains and losses (Table 2). On the other hand, almost no imbalances in common could be found for soft tissue sarcoma (Table 2).

Table 2. Copy number changes associated with molecular subtypes of human sarcomas according to references (Forus *et al.*, 1995; Mihic-Probst *et al.*, 2004; Deeb *et al.*, 2005), compared with the copy number variants (CNVs) in cell line TSC2ang1. Concordances with human CNVs are highlighted in bold; loss or gain in brackets means that this aberration has been seen in the tumor type, but not that frequently.

chromosomal region	**TSC2ang1**	**soft tissue sarcoma (Forus *et al.*, 1995)**	**Undiff. high grade pleomorphic sarcoma (Mihic-Probst *et al.*, 2004)**	**Myeloid sarcoma (Deeb *et al.*, 2005)**
1pter-p31.1	loss	gain	no CNV	loss
2p16-q32.1	loss	no CNV	(loss)	no CNV
3pter-qter	loss	no CNV	(loss)	no CNV
4p15.2-q22	loss	no CNV	loss or gain	no CNV
5pter-p15.2	loss	no CNV	(loss)	gain
5q11-q15	loss	no CNV	(loss)	loss
5q31.1	gain	no CNV	loss	loss
5q33.2-qter	loss	no CNV	loss	loss
6pter-p22.1	gain	gain	no CNV	loss
6q15-q16.3	gain	no CNV	loss	no CNV
7p13-q21.3	loss	gain	no CNV	loss
8p23.1-p12	loss	no CNV	(loss)	gain
8q12	gain	no CNV	gain	gain
8q21.3-q22.1	gain	gain	gain	gain
9p23-p21.3	loss	no CNV	loss	no CNV
9p21.1-p13	gain	no CNV	loss	no CNV
9q21.33-q32	gain	gain	(gain)	no CNV
9q33-qter	loss	gain	(gain)	loss
10pter-p15	gain	no CNV	no CNV	no CNV
10p14-qter	loss	no CNV	loss	loss
11pter-qter	loss	gain	loss	loss
12pter-p11	loss	no CNV	loss	(loss)
12q24.1-qter	loss	gain	gain	(loss)
13q14.1-qter	loss	no CNV	loss	loss
14q11.2	loss	no CNV	no CNV	loss
14q22	loss	no CNV	no CNV	loss
15q11.1-qter	loss	gain	no CNV	(loss)
16pter-qter	loss	no CNV	loss	loss
17pter-qter	loss	no CNV	gain	loss
19q12-qter	loss	no CNV	no CNV	loss
20pter-qter	loss	no CNV	no CNV	(loss)
21p11.1-qter	loss	no CNV	no CNV	(loss)
22q11.2-q12	loss	no CNV	no CNV	loss
OVERALL	33	18/33	18/33	19/33

4. Discussion and conclusion

TSC2ang1 cell line was established form a tsc2+/-mouse being heterozygous for tuberin. This mouse had most likely a karyotype 20,XY or 20,YN. It was never tested if the tsc2 gene knockout led to any chromosomal changes in the host strain (Onda *et al.*, 1999). The first sold stain cytogenetic analyses in TSC2ang1 already revealed a near tetraploid karyotype with-compared to the present results with two clones-at least three clones (Wlodarski *et al.*, 2008). Besides clone 1 without any "Robertsonian translocation"-like chromosomes, Wlodarski *et al.* (2008) found also clone 2 with two "Robertsonian translocation"-like chromosomes, in the present study characterized as idic(11)(A), and dic(16,18)(A1;A1). In 2008 (Wlodarski *et al.*, 2008) clone 1 constituted ~52% of the TSC2ang1 cell line and clone 2 only ~6% of them. Besides, at that time 48% had either the idic(11)(A) or the dic(16,18)(A1;A1), exclusively, forming a clone 3, which was absent in the actual study. Thus, clone 1 kept its original size from 2008 onwards, while clone 2 repressed and replaced clone 3 completely and expanded from 6% to ~50% of the cells. As highlighted in Table 1 different imbalances present in both clones could be characterized by CMA and assigned to one of the two clones. Interestingly, besides the loss of one tsc2 copy by genetic engineering of the original mouse strain from which the tumor was derived, clone 2 additionally lost a tsc2 copy due to dic(16,18)(A1;A1) formation.

Both clones of cell line TSC2ang1 are near-tetraploid (Figure 1); thus all copy number alterations highlighted in Figure 2 and Tables 1 and 2 refer just to 25% of gain or loss of chromosomal material; only the 4A1-4C1-region in clone 1 had overall six copies with a 50% gain. Polyploidization is rather the rule than the exception in previously studied murine tumor cell lines (Table 3): only 6/25 studied lines (24%) remained diploid, while the remainder 19 (= 76%) lines became triploid (6 lines = 24%), tetraploid (12 line = 48%) or even pentaploid (1 line = 4%) (Kubicova *et al.*, 2017; Leibiger *et al.*, 2013; Guja *et al.*, 2017; Azawi *et al.*, 2020, 2021a-2021d, 2022, Manferrari *et al.*, 2020; Piaszinski *et al.*, 2021, Rhode *et al.*, 2018; Steinacker *et al.*, 2021; Wahlbuhl *et al.*, 2020). Still, it has to be considered, that polyploidization seems to be rather a cell culture effect, than a reflection of the original tumor karyotype (Davoli & de Lange, 2012). This has to be considered in all studies such cell lines are applied for. Also it is interesting that 16/25 murine tumor cell lines summarized in Table 3 (64%) loose in culture one to half of their sex chromosomes, while only in two of them one or two Y-chromosomes are gained.

Table 3. Results of present and previous comparable studies in murine tumor cell lines highlighting their ploidy grade and presence or absence of 50% of sex chromosomes-if sex chromosomes were involved in rearrangements this was not further considered here.

Cell line	Tumor type	Ploidy	Sex chrs.	Reference
A-20	Burkitt's lymphoma	~x2	X,-X or-Y	Guja *et al.*, (2017)
MMT 060562	Breast cancer	~x2	XX	Azawi *et al.*, (2020)
TA3 Hauschka	Breast cancer	~x2	XX	Azawi *et al.*, (2020)
AE17	Mesothelioma	~x2	XX	Kubicova *et al.* (2017)
C57/B1	Melanoma	~x2	X,-X or-Y	Manferrari *et al.* (2020)
WR21	Salivary gland cancer	~x2	XY,+Y	Steinacker *et al.* (2019)
EMT6/P	Breast cancer	~x3	XX,-X	Azawi *et al.*, (2020)
MH-22A	Liver cancer	~x3	XX,-X or-Y	Azawi *et al.*, (2021b)
Hepa 1-6	Liver cancer	~x3	XXX	Azawi *et al.*, (2021b)
AC29	Mesothelioma	~x3	XXX	Wahlbuhl *et al.* (2020)
CMT-93	Colorectal cancer	~x3	XXY	Rhode *et al.*, (2018)
CT26	Colorectal cancer	~x3	XX,-X or-Y	Rhode *et al.*, (2018)
JC	Breast cancer	~x4	XX,-X,-X	Azawi *et al.*, (2021c)
KLN 205	tracheal squamous cell carcinoma	~x4	XXYY,+Y,+Y	Azawi *et al.*, (2021a)
LA-4	squamous cell lung cancer	~x4	XX,-X,-X	Azawi *et al.*, 2021d)
AB1	Mesothelioma	~x4	XX,-X,-X	Wahlbuhl *et al.* (2020)
AB22	Mesothelioma	~x4	XX,-X,-X	Wahlbuhl *et al.* (2020)
NIH 3T3	Ectodermal cancer	~x4	XXY,-Y	Leibiger *et al.* (2013)
B16-F0	Melanoma	~x4	XX,-X,-X or-Y,-Y	Azawi *et al.* (2022)
S91 Clone M3	Melanoma	~x4	XXXX	Piaszinski *et al.* (2021)
B16-F1	Melanoma	~x4	XX,-X,-X or-Y,-Y	Piaszinski *et al.* (2021)
B16-4A5	Melanoma	~x4	XX,-X,-X or-Y,-Y	Piaszinski *et al.* (2021)
SCA-9	Salivary gland cancer	~x4	XX,-X,-X or-Y,-Y	Steinacker *et al.* (2019)
TSC2ang1	Sarcoma	~x4	XX,-X,-X or-Y,-Y	This study
C-127I	Breast cancer	~x5	XXX,-X,-X	Azawi *et al.*, (2020)

The cell line TSC2ang1 for the present study has been purchased from ATCC in 2014, was directly cultivated and worked up, and afterwards stored at-196°C since then. However, during last 8 years the TSC2ang1 cells at the provider may have been further undergone karyotype evolution during cultivations; thus, it is recommended that a CMA or a cytogenetic study is done to confirm / compare with the chromosomal/ genetic constitution that is reported in the present study prior to further experiments.

TSC2ang1 cells are derive from a cutaneous sarcoma (Onda *et al.*, 1999); as

the cells have a tsc2 gene deletion (most likely two to three active copies of tsc2 gene in clone 1 and only one to two active copies in clone 2) it was suggested in 2008 they could be a good and 'the only available' model for TS-associated skin lesions, i.e. hamartomas (Wlodarski *et al.*, 2008). However, the results comparing TSC2ang1 imbalances with such of undifferentiated high grade pleomorphic, myeloid and soft tissue sarcoma (Table 2) suggested that this cell line is rather a model for skin sarcoma, than for non-malignant hamartomas. This is also supported by the finding that there are no CMA based studies available showing chromosomal gains or losses in hamartomas.

In conclusion, TSC2ang1 cell line is-concerning its cytogenomic signature-a typical sarcoma. The fact that tsc2 gene was knocked out in the original mouse strain seems to be less important in these near tetraploid cells with two genetically different cell clones. In future, it might be of interest to separate clone 1 and clone 2 from each other by single cell cultivation and characterize their potentially different cellular features.

5. Acknowledgement

The technical support from Dr Nadezda Kosyakova (Jena University Hospital, Friedrich Schiller University, Institute of Human Genetics, Jena, Germany) is gratefully acknowledged.

6. References

Alesi, N., Akl, E.W., Khabibullin, D., Liu, H.J., Nidhiry, A.S., Garner, E.R., Filippakis, H., Lam, H.C., Shi, W., Viswanathan, S.R., Morroni, M., Ferguson-Smith, M. & Henske, E.P. (2021). TSC2 regulates lysosome biogenesis via a non-canonical RAGC and TFEB-dependent mechanism. *Nature Communications, 12*(1), 4245. https://doi.org/10.1038/s41467-021-24499-6.

Alkharusi, A., Lesma, E., Ancona, S., Chiaramonte, E., Nyström, T., Gorio, A. & Norstedt, G. (2016). Role of prolactin receptors in lymphangioleiomyomatosis. *PLoS One, 11*(1), e0146653. https://doi.org/10.1371/journal.pone.0146653.

Azawi, S., Liehr, T., Rincic, M. & Manferrari, M. (2020). Molecular cytogenomic characterization of the murine breast cancer cell lines C-127I, EMT6/P and TA3 Hauschka. *International Journal of Molecular Sciences, 21*(13), 4716. https://doi.org /10.3390/ijms2113471 6.

Azawi, S., Liehr, T. & Rincic, M. (2021a). First molecular cytogenetic characterization of tracheal squamous cell carcinoma cell line KLN 205. *Journal of Cancer and Metastasis Treatment, 7*(1), 38. https://doi.org/10.20517/2394-4722.2021.59.

Azawi S., Barf L-M. & Liehr, T. (2021b). First molecular cytogenetic characterization of the MMT 060562 murine breast cancer cell line. *Research Results in Biomedicine, 7*(1), 4-14. http://rrmedicine.ru/en/journal/article/2278/.

Azawi, S., Piaszinski, K., Balachandran, M., Liehr, T. & Rincic, M. (2021c). Molecular cytogenomic characterization of two murine liver cancer cell lines: MH-22A and Hepa 1-6. *Journal of Genetics and Genomes, 5*(1), 1. https://www.hilarispublisher.com/open-access/molecular-cytogenomic-characterization-of-two-murine-liver-cancer-cell-lines-mh22a-and-hepa-16.pdf.

Azawi, S., Rincic, M. & Liehr, T. (2021d). Cytogenomic characteristics of murine breast cancer cell line JC. *Molecular Cytogenetics, 14*(1), 7. https://doi.org/10.1186/s13039-020-00524-z.

Azawi, S., Balachandran, M., Kramer, F., Kankel, S., Rincic, M. & Liehr, T. (2022). Molecular cytogenetic characterization of the urethane-induced murine lung cell line LA-4 as a model for human squamous cell lung cancer. *Molecular Clinical Oncology, 16*(1), 9. https://doi.org /10.3892/mco.2021.2440.

Davoli, T. & de Lange, T. (2012). Telomere-driven tetraploidization occurs in human cells undergoing crisis and promotes transformation of mouse cells. *Cancer Cells, 21*(6), 765-776. https://doi.org /10.1016 /j.ccr.2012.03.044.

Deeb, G., Baer, M.R., Gaile, D.P., Sait, S.N., Barcos, M., Wetzler, M., Conroy, J.M., Nowak, N.J., Cowell, J.K. & Cheney, R.T. (2005). Genomic profiling of myeloid sarcoma by array comparative genomic hybridization. *Genes Chromosomes and Cancer, 44*(4), 373-383. https://doi.org/10.1002/gcc.20239.

European Chromosome 16 Tuberous Sclerosis Consortium . (1993). Identification and characterization of the tuberous sclerosis gene on chromosome 16. *Cell, 75*(7), 1305-1315.

Ferreira, R.B., Wang, M., Law, M.E., Davis, B.J., Bartley, A.N., Higgins, P.J., Kilberg, M.S., Santostefano, K.E., Terada, N., Heldermon, C.D., Castellano, R.K. & Law, B.K. (2017). Disulfide bond disrupting agents activate the unfolded protein response in EGFR-and HER2-positive breast tumor cells. *Oncotarget, 8*(17), 28971-28989. https://doi.org/10.18632/oncotarget.15952.

Forus, A., Weghuis, D.O., Smeets, D., Fodstad, O., Myklebost, O. & van Kessel, A.G. (1995). Comparative genomic hybridization analysis of human sarcomas: I. Occurrence of genomic imbalances and identification of a novel major amplicon at 1q21-q22 in soft tissue sarcomas. *Genes Chromosomes and Cancer, 14*(1), 8-14. https://doi.org /10.1002/gcc.2870140103.

Gao, Y., Gartenhaus, R.B., Lapidus, R.G., Hussain, A., Zhang, Y., Wang, X. & Dan, H.C. (2015). Differential IKK/NF-κB activity is mediated by TSC2 through mTORC1 in PTEN-null prostate cancer and tuberous sclerosis complex tumor cells. *Molecular Cancer Research, 13*(12), 1602-1614. https://doi.org /10.1158/1541-7786.mcr-15-0213.

Govindarajan, B., Willoughby, L., Band, H., Curatolo, A.S., Veledar, E., Chen, S., Bonner M.Y., Abel, M.G., Moses, M.A. & Arbiser, J.L. (2012). Cooperative benefit for the combination of rapamycin and imatinib in tuberous sclerosis complex neoplasia. *Vascular Cell, 4*(1), 11. https://doi.org /10.1186 /2045-824x-4-11.

Guja, K., Liehr, T., Rincic, M., Kosyakova, N. & Azawi, S.S.H. (2017). Molecular cytogenetic characterization identified the murine B-cell lymphoma cell line A-20 as a model for sporadic Burkitt's lymphoma. *Journal of Histochemistry and Cytochemistry, 65*(11), 669-677. https://doi.org /10.1369/ 0022155417731319.

Kubicova, E., Trifonov, V., Borovecki, F., Liehr, T., Rincic, M., Kosyakova, N. & Hussein, S.S. (2017). First molecular cytogenetic characterization of murine malignant mesothelioma cell line AE17 and in silico translation to the human genome. *Current Bioinformatics, 12*(1), 11-18. http://dx.doi.org/ 10.2174 /1574893611666160606164459.

Leibiger, C., Kosyakova, N., Mkrtchyan, H., Glei, M., Trifonov, V. & Liehr, T. (2013). First molecular cytogenetic high resolution characterization of the NIH 3T3 cell line by murine multicolor banding. *Journal of Histochemistry and Cytochemistry, 61*(4), 306-312. https://doi.org /10.1369/0022155413476868.

Luo, C, Ye, W. R., Shi, W., Yin, P., Chen, C., He, Y.B., Chen, M .F., Zu, X.B. & Cai, Y. (2022). Perfect match: mTOR inhibitors and tuberous sclerosis complex. *Orphanet Journal of Rare Diseases, 17*(1), 106. https://doi.org/10.1186/ s13023-022-02266-0.

Manferrari, M., Rincic, M., Liehr, T. & Azawi, S. (2020). Cytogenomics of murine melanoma cell lines C57/ B1 and B16-F0. *Molecular and Experimental Biology in Medicine, 3*(2), 39-44. https://hrcak.srce.hr/ file/380456.

Mihic-Probst, D., Zhao, J., Saremaslani, P., Baer, A., Oehlschlegel, C., Paredes, B., Komminoth, P. & Heitz, P.U. (2004). CGH analysis shows genetic similarities and differences in atypical fibroxanthoma and undifferentiated high grade pleomorphic sarcoma. *Anticancer Research, 24*(1), 19-26. https://ar.iiarjournals.org/content/ anticanres/24/1/19.full.pdf.

Onda, H., Lueck, A., Marks, P.W., Warren, H. B. & Kwiatkowski, D.J. (1999). Tsc2(+/-) mice develop tumors in multiple sites that express gelsolin and are influenced by genetic background. *Journal of Clinical Investigations, 104*(6), 687-695. https://doi.org/10.1172/jci7319.

Piaszinski, K., Rincic, M., Liehr, T. & Azawi, S. (2021). Molecular cytogenetic characterization of the murine melanoma cell lines S91 clone M3 and B16-F1 with variant B16-4A5. *Cytogenetics and Genome Research, 161*(1-2), 82-92. https://doi.org/10.1159/000513174.

Rhode, H., Liehr, T., Kosyakova, N., Rinčic, M. & Azawi, S.S.H. (2018). Molecular cytogenetic characterization of two murine colorectal cancer cell lines. *OBM Genetics, 2*(3), 1803037. http://dx.doi.org/10.21926/obm.genet.1803037.

Steinacker, R., Liehr, T., Kosyakova, N., Rincic, M. & Azawi, S.S.H. (2019). Molecular cytogenetic characterization of two murine cancer cell lines derived from salivary gland. *Biological Communications, 63*(4), 243-255. https://doi.org/10.21638/spbu03.2018.403.

Swarbrick, A. W., Frederiks, A.J. & Foster, R.S. (2021). Systematic review of sirolimus in dermatological conditions. *Australasian Journal of Dermatology, 62*(4), 461-469. https://doi.org/10.1111/ajd.13671.

Van Slegtenhorst, M., de Hoogt, R., Hermans, C., Nellist, M., Janssen, B., Verhoef, S., Lindhout, D., van den Ouweland, A., Halley, D., Young, J., Burley, M., Jeremiah, S., Woodward, K., Nahmias, J., Fox, M., Ekong, R., Osborne, J., Wolfe, J., Povey, S., Snell, R.G., Cheadle, J.P., Jones, A.C., Tachataki, M., Ravine, D., Sampson, J.R., Reeve, M.P., Richardson, P., Wilmer, F., Munro, C., Hawkins, T.L., Sepp, T., Ali, J.B., Ward, S., Green, A. J., Yates, J.R., Kwiatkowska, J., Henske, E.P., Short, M.P., Haines, J.H., Jozwiak, S. & Kwiatkowski, D.J. (1997). Identification of the tuberous sclerosis gene TSC1 on chromosome 9q34. *Science 277*(5327), 805-808. https://doi.org/10.1126/science.277.5327.805.

Wahlbuhl, E., Liehr, T., Rincic, M. & Azawi, S. (2020). Cytogenomic characterization of three murine malignant mesothelioma tumor cell lines. *Molecular Cytogenetics, 13*(1), 43. https://doi.org/10.1186/s13039-020-00511-4.

Wlodarski, P.K., Maksym, R., Oldak, M., Jozwiak, S., Wojcik, A., & Jozwiak, J. (2008). Tuberin-heterozygous cell line TSC2ang1 as a model for tuberous sclerosis-associated skin lesions. *International Journal of Molecular Medicine, 21*(2), 245-250. https://doi.org/10.3892/ijmm.21.2.245.